Chapter 3

Incorporation of PPE in Lamellar Self-Assembled PS-*b*-P4VP(PDP) Supramolecules and PS-*b*-P4VP Diblock Copolymers

Self-assembled blends of PS-b-P4VP(PDP) supramolecules, obtained by hydrogen bonding of pentadecylphenol (PDP) side chains to the poly(4-vinylpyridine) (P4VP) block of a block copolymer of polystyrene (PS) and P4VP, and poly(2,6-dimethyl-1,4-diphenyl oxide) (PPE) were investigated by thermal analysis and small-angle X-ray scattering (SAXS) and compared with blends of pure PS-b-P4VP and PPE. Differential scanning calorimetry (DSC) measurements showed a single composition dependent T_g of the

PPE/PS layers for both systems, demonstrating that PPE is distributed throughout the PS layers. Furthermore, DSC showed that for the PPE/PS-b-P4VP(PDP) blends the presence of PDP is not restricted to the P4VP layers. Its partial presence in the PS-containing domains was confirmed by nuclear magnetic resonance (NMR) spectroscopy on PS-P4VP core-corona nanorods prepared from hexagonally self-assembled PS-b-P4VP(PDP) supramolecules. The results of the SAXS study on the dependence of the lamellar period of PPE/PS-b-P4VP blends on the amount of PPE were in excellent agreement with a theoretical model based on the Alexander-De Gennes approximation assuming a uniform distribution of PPE throughout the PS layers. For PPE/PS-b-P4VP(PDP) blends the dependence of the long period on the amount of PPE turned out to be somewhat stronger, which may be related to the supramolecular comb-shaped nature of the P4VP(PDP) blocks.

3.1 Introduction

The combination of block copolymer self-assembly and supramolecular chemistry is a promising method to achieve nanoscale structuring in materials and therefore a key ingredient for nanotechnology of soft materials.[1-14] Morphology and domain sizes can easily be controlled by adjusting the pertinent parameters such as composition, molar mass, etc. Simple examples, that are related to the subject of the previous as well as the present chapter, include the production of nanoporous membranes and nano-objects, which can readily be acquired by selectively removing one of the blocks of suitably self-assembled block copolymer systems.[15-17] The comb-shaped supramolecules route, where short side chains are attached by hydrogen bonding to one of the blocks of a diblock copolymer only to be removed by dissolution after the self-assembly process has been completed, enhances the possibilities for the production of these materials.[12-14,18] In particular, core-corona nanorods can be easily prepared in this way with the core being formed by the majority (longest) rather than the minority block of the diblock copolymer used.[18,19] In the previous chapter, it was demonstrated that nanorods with a PS core and a P4VP corona, obtained via the comb-shaped supramolecules route, exhibit very poor mechanical properties. The rods consisted of nearly symmetric PS-*b*-P4VP diblock copolymers with a molar mass of ca. 20000 g mol^{-1} for each block, and the poor mechanical properties were attributed to the absence of entanglements. Addition of a sufficient amount of PPE, which is well-known for its excellent thermodynamic miscibility with PS,[20] to the PS core introduced entanglements, resulting in nanorods with much better

properties, that can be used as templates for e.g. transition metal oxide tubes.[21,21]

Blends of block copolymers with homopolymers that have a specific exothermic interaction with one of the blocks of the block copolymers have been investigated in the past by different groups.[23-27] In several studies PS-based block copolymers were combined with PPE. Paul and co-workers[26,27] used polystyrene-*block*-polybutadiene-*block*-polystyrene (SBS) triblock copolymers, whereas Hashimoto and co-workers[28] used polystyrene-*block*-polyisoprene (PS-*b*-PI) diblock copolymers. In all cases an increased solubilization of PPE in the PS domains, as compared to the solubilization of homopolymer PS, was observed. If lamellar self-assembled diblock copolymers are mixed with a homopolymer that is chemically identical to one of the blocks, the spatial distribution of the homopolymer depends on its relative molar mass. For low molar masses, the homopolymer will be distributed uniformly throughout the layers of the corresponding block. For a molar mass of the homopolymer that is comparable to that of the corresponding block, the homopolymer will be confined to the center of the layers, i.e., segregated in the midplane. A significantly higher molar mass of the homopolymer finally leads to macrophase separation.[7,28-31] For the above-mentioned systems with PPE, on the other hand, the effect of the molar mass of PPE was found to be small or nonexistent, which can be ascribed to the favorable interaction between PS and PPE.[20]

In the study on PPE reinforcement of PS-P4VP core-corona nanorods, the fraction of PPE required to introduce entanglements was therefore estimated assuming a uniform distribution of PPE in the PS cylinders of self-assembled PS-*b*-P4VP complexes with dodecylphenol (DDP) or pentadecylphenol (PDP). P4VP(PDP) combs self-assemble in a lamellar morphology below the T_{ODT}, which is well above room temperature. In the case of DDP the alkyl tail is too small to give rise to self-assembly of the P4VP(DDP) matrix even at temperatures as low as room temperature, besides this however, the behavior of PDP and DDP related systems is comparable. In the present chapter the thermal and morphological properties of lamellar-*in*-lamellar self-assembled blends of PPE/PS-*b*-P4VP(PDP) are addressed and compared with systems without PDP, i.e., PPE/PS-*b*-P4VP in order to determine if the assumption of a uniform distribution of PPE within the PS core of the nanorods was correct. DSC was used to characterize the thermal properties. With SAXS the long period was determined as a function of the amount of PPE added and analyzed using a simple Alexander-De Gennes model. In agreement with the above-mentioned studies on different PS-based block copolymers, PPE was found to be distributed throughout the PS lamellae, even though the PPE used has a larger molar mass than the PS blocks. In addition, the

DSC data indicate that PDP is not exclusively confined to the P4VP domains but that a significant amount is present in the PPE/PS phase as well, leading to a substantial glass transition temperature depression. The corresponding increase in mobility of the PPE/PS domains is of direct interest for the large-amplitude oscillatory shear procedures that are applied to macroscopically align self-assembled PPE/PS-*b*-P4VP(PDP) systems.[19,32-34] The presence of PDP in the PS layers, concluded from the DSC data, was verified by NMR on PS-*b*-P4VP core-corona nanorods prepared from hexagonally ordered PS-*b*-P4VP(PDP) supramolecules. In the preparation process of the nanorods all the PDP is removed from the P4VP matrix, and any PDP left resides in the glassy PS core.

3.2 Experimental section

3.2.1 Materials and sample preparation

Chemicals. Three different block copolymers of PS and P4VP with comparable molar mass of the PS blocks were obtained from Polymer Source, Inc.: P103-S4VP (M_n(PS) = 19600 g mol^{-1}, M_n(P4VP) = 5100 g mol^{-1}, M_w/M_n = 1.08), P105-S4VP (M_n(PS) = 21400 g mol^{-1}, M_n(P4VP) = 20700 g mol^{-1}, M_w/M_n = 1.13), and P3546-S4VP (M_n(PS) = 20000 g mol^{-1}, M_n(P4VP) = 19000 g mol^{-1}, M_w/M_n = 1.09). The polymers were used as received. 3-*n*-Pentadecylphenol (PDP) was purchased from Aldrich and was recrystallized twice from petroleum ether (40-60 w/w) and dried in a vacuum at 40 °C. PPE was purchased from Polymer Source, Inc. (M_n = 25700 g mol^{-1}, M_w/M_n = 1.37) and was reprecipitated from chloroform/methanol before using.

Sample preparation. To obtain the PPE/PS-*b*-P4VP(PDP) blends, PS-*b*-P4VP, PDP (in a stoichiometrical amount with respect to the number of pyridine groups), and PPE were dissolved in analytical grade chloroform. The concentration of polymer was kept below 2 wt% to ensure homogeneous complex formation, and the solutions were stirred for 2 h. The solutions were then dried in air within a few hours, and final drying was performed at 40 °C in a vacuum for at least 2 days. Systems without PDP were obtained in a similar fashion. All systems used are listed in Table 3.1 and, except for P105(PDP) which self-assembles in the form of hexagonally ordered cylinders of PS in a matrix of P4VP(PDP), are expected to form a lamellar morphology as can be deduced from the P4VP and comb weight fractions.[35]

Table 3.1. Characterization of systems studied

Sample	w_{PPE} [a]	w [b]	w_{P4VP} [c] resp. w_{comb} [d]
P3546	0	0	0.487
P3546/$PPE_{0.10}$	0.10	0.054	0.461
P3546/$PPE_{0.20}$	0.20	0.114	0.432
P3546/$PPE_{0.30}$	0.30	0.180	0.399
P3546/$PPE_{0.35}$	0.35	0.216	0.382
P105(PDP)			0.790
P103(PDP)	0	0	0.503
P103(PDP)/$PPE_{0.10}$	0.10	0.052	0.477
P103(PDP)/$PPE_{0.20}$	0.20	0.110	0.448
P103(PDP)/$PPE_{0.30}$	0.30	0.175	0.415
P103(PDP)/$PPE_{0.40}$	0.40	0.249	0.378

[a] w_{PPE} = *weight fraction of PPE in the PS/PPE phase.* [b] w = *weight fraction of PPE in the entire system.* [c] w_{P4VP} = *weight fraction of P4VP in the entire system.* [d] w_{comb} = *weight fraction of P4VP(PDP) combs in the entire system if all PDP were in the P4VP domains.*

3.2.2 Instrumental methods

Differential Scanning Calorimetry. Temperature-modulated scanning calorimetry was performed using a DSC Q1000 (TA Instruments). All samples were heated with a rate of 1 °C min^{-1}, an oscillation amplitude of 1 °C, and an oscillation period of 60 s. Samples were first equilibrated at -30 °C, heated to 180 °C, cooled to -30 °C, and then heated again to 180 °C. Data were taken from the second heating.

Small-Angle X-ray Scattering. For SAXS, the samples were heated (PPE/PS-*b*-P4VP systems to 180 °C and PPE/PS-*b*-P4VP(PDP) systems to 120 °C) in a mold of 14 mm diameter and 1 mm thickness. For 15 min the samples were allowed to flow to fill the mold while applying slight pressure, after which the press was cooled with cooling water before removing the tablets from the press. A small piece of the tablets was cut off for measurements.

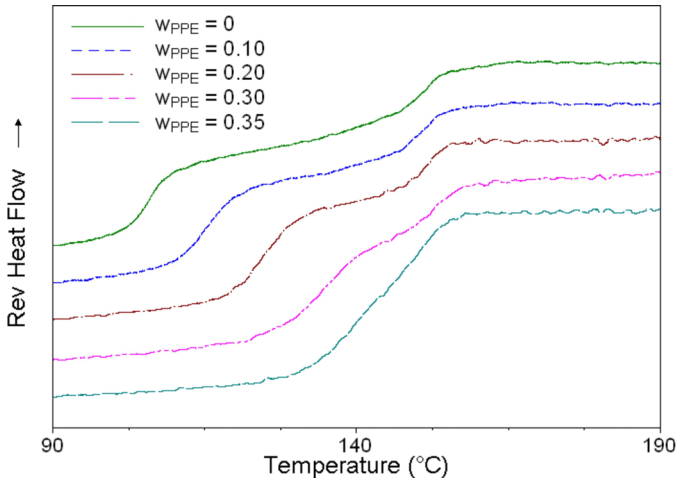

Figure 3.1. DSC curves of P3546/PPE blends with different amounts w_{PPE} of PPE. Rather than the total heat flows, the reversing heat flows are shown for clarity, as the T_g positions are more pronounced in these curves.

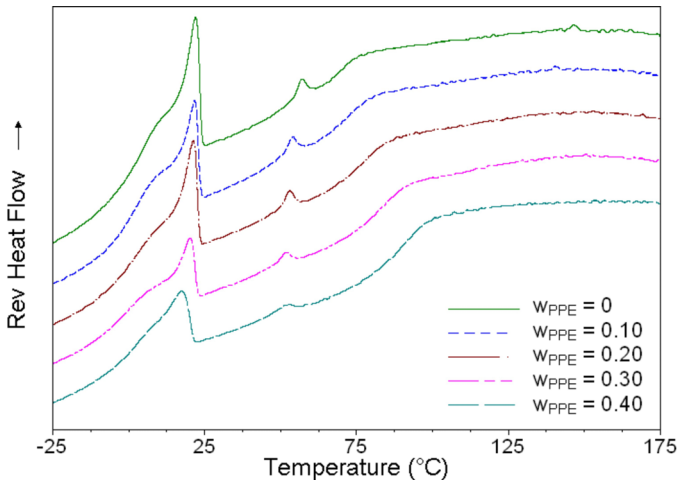

Figure 3.2. DSC curves of P103(PDP)/PPE blends with different compositions, showing melting of PDP, the ODT of P4VP(PDP) and the T_g of PS/PPE.

SAXS measurements were carried out at room temperature using a NanoStar camera (Bruker and Anton Paar). A ceramic fine-focus X-ray tube, powered with a Kristallflex K760 generator at 35 kV and 40 mA, has been used in point focus mode. The primary X-ray flux is collimated using cross-coupled Göbel mirrors and a pinhole of 0.1 mm diameter, providing a Cu Kα radiation beam with a full width at half-maximum of about 0.2 mm at the sample position. The sample-detector distance was 1.06 m. The scattering intensity was registered by a Hi-Star position-sensitive area detector (Siemens AXS) in the *q* range of 0.1-2.0 nm^{-1}. The scattering vector q is defined as $q = (4\pi/\lambda) \sin(\theta/2)$, where $\lambda = 0.1542$ nm and θ is the scattering angle. The measuring time for most samples was 1 h.

Nuclear Magnetic Resonance spectroscopy. According to the procedure described in the previous chapter, the P105(PDP) system was aligned using large-amplitude oscillatory shear. After this, part of the material was placed in a dialysis tube (SERVAPOR, cutoff M = 12000, Serva) filled with ethanol and dialyzed against ethanol for 2 weeks. After 1 week, the solvent was replaced. The nanorods were collected from the bottom of the obtained nanorod suspension, and residual ethanol was allowed to evaporate off in a vacuum at 40 °C overnight. The remaining nanorods were redissolved in deuterated chloroform. ^{1}H NMR spectra were obtained using a 300 MHz Varian NMR spectrometer.

3.3 Results and discussion

3.3.1 Thermal analysis

The thermal behavior of the blends of the symmetric diblock copolymer P3546 (M_n(PS) = 20000, M_n(P4VP) = 19000) with PPE is given in Figure 3.1. The pure block copolymer shows two T_g's, one at 106 °C and the other at 152 °C, corresponding to the PS and P4VP layers. When adding PPE, the lower T_g shifts to higher values, whereas the T_g of the P4VP layers exhibits no notable change and at higher temperatures ($T \leq$ 240 °C) a separate T_g of PPE is not observed. For the highest amount of PPE added, $w_{PPE} = 0.35$, the T_g's of the PS/PPE and P4VP layers overlap. The fact that the T_g of the P4VP layers is unaffected implies that PPE is selectively dissolved in the PS phase. The absence of PPE in the P4VP phase has to be expected. A recent study on the miscibility of random copolymers of styrene and 4-vinylpyridine, P(S-*rand*-4VP), with PPE showed that the interaction between PPE and P4VP is even more unfavorable than that between PS and P4VP.[36] From a similar miscibility

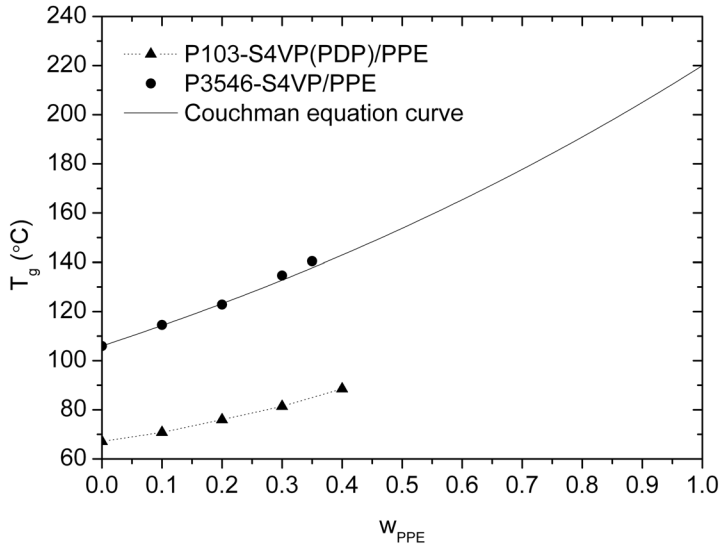

Figure 3.3. Graph of the T_g of PS/PPE in P3546/PPE and P103(PDP)/PPE as a function of the weight fraction of PPE in the PS/PPE phase.

study on blends of P(S-*rand*-4VP) and PS the Flory-Huggins parameter of the latter was found to satisfy $0.30 < \chi_{S,4VP} \leq 0.35$.[37]

The PDP-containing systems, except for one, involve the highly asymmetric diblock copolymer P103 (M_n(PS) = 19600, M_n(P4VP) = 5100) in order that the weight fraction of the P4VP(PDP) block of the PS-*b*-P4VP(PDP) supramolecules is ~0.5 (see Table 3.1). In all cases PDP is present in a stoichiometric amount with respect to the number of pyridine groups. On addition of PPE, the microphase separation between the PS/PPE domains and the P4VP(PDP) domains results in a lamellar morphology for weight fractions as high as $w_{PPE} = 0.40$. Apart from the lamellar microphase separation between PS/PPE and P4VP(PDP), the P4VP(PDP) combs self-assemble in a lamellar morphology below the T_{ODT}, which is at ca. 57 °C for pure PS-*b*-P4VP(PDP), thus leading to the well-known hierarchical structures.[38,39] Furthermore, the PDP side chains crystallize at temperatures below ca. 20 °C.[40] The DSC measurements of these systems, presented in Figure 3.2, clearly reveal the various transitions. Again, the reversing heat flows are shown for clarity. In all cases, the total heat flow showed the same characteristics as the reversing heat flow. First, around room temperature the melting endotherm of PDP is

observed. Its complex shape is believed to be due to the presence of different crystal modifications. On further heating the endotherm due to the order-disorder transition (ODT) of the P4VP(PDP) domains is found, and finally the T_g of the PS/PPE phase appears. Measurements to higher temperatures (T ≤ 240 °C) did not show a separate T_g for PPE. As indicated in the previous chapter, the T_g of P4VP is strongly suppressed due to the presence of the side chains and is expected to be situated under the PDP melting peak.[40]

The glass transition temperatures of the PS/PPE layers are summarized in Figure 3.3. In blends of PPE and the symmetric diblock copolymer P3546, the T_g of the PS/PPE layers steadily increases as a function of the amount of PPE. The solid line through the experimental points is calculated according to the Couchman expression[41,42]

$$T_g = \frac{w_{PS}\Delta C_{p,PS}T_{g,PS} + w_{PPE}\Delta C_{p,PPE}T_{g,PPE}}{w_{PS}\Delta C_{p,PS} + w_{PPE}\Delta C_{p,PPE}} \quad (1)$$

where ΔC_p denotes the incremental change in specific heat of the respective pure components ($\Delta C_{p,PS}$ = 30.7 J mol^{-1} K^{-1}, $\Delta C_{p,PPE}$ = 31.9 J mol^{-1} K^{-1})[43] and w denotes their weight fraction. $T_{g,PPE}$ is taken to be 220 °C, the value measured for the PPE homopolymer used. The fit is excellent, thereby demonstrating that the PS/PPE layers in the lamellar self-assembled PPE/P3546 behave very much like a simple PS/PPE homopolymer mixture. In the latter case the validity of eq. 1 has been amply demonstrated.[42-44] The same has found to hold for blends of PPE and polystyrene-*block*-poly(ethylene-butylene)-*block*-polystyrene (SEBS) triblock copolymers.[43]

The results for the blends of PS-*b*-P4VP(PDP) supramolecules with PPE are considerably different. Whereas, as before, the T_g of PS/PPE shifts to higher values for a larger weight fraction of PPE, the actual values are much lower. The pure PS-*b*-P4VP(PDP) supramolecules system shows a T_g of the PS layers of only 67 °C instead of 106 °C (Figure 3.3). This depression results from the additional presence of PDP in the PS phase as the following experiment shows. The symmetric P105 diblock copolymer was used to prepare PS-*b*-P4VP(PDP) supramolecules that self-assemble as hexagonally ordered PS cylinders inside a P4VP(PDP) matrix. After alignment by large-amplitude oscillatory shear, PS-*b*-P4VP core-corona nanorods were prepared by dissolving the PDP from the matrix. This well-known procedure can be recalled from Chapter 2.

Because ethanol is a non-solvent for PS, it is likely that PDP is not easily washed out of the nanorod cores during dissolution of PDP. The nanorods thus produced were investigated by Fourier transform infrared (FTIR) spectroscopy and NMR. The FTIR data were inconclusive; however, NMR clearly revealed the presence of PDP (Figure 3.4). Additional DSC measurements on mixtures of a PS homopolymer mixed with different amounts of PDP showed that the presence of 5% w/w PDP resulted in a glass transition temperature depression to ca. 65 °C. Hence, we can safely

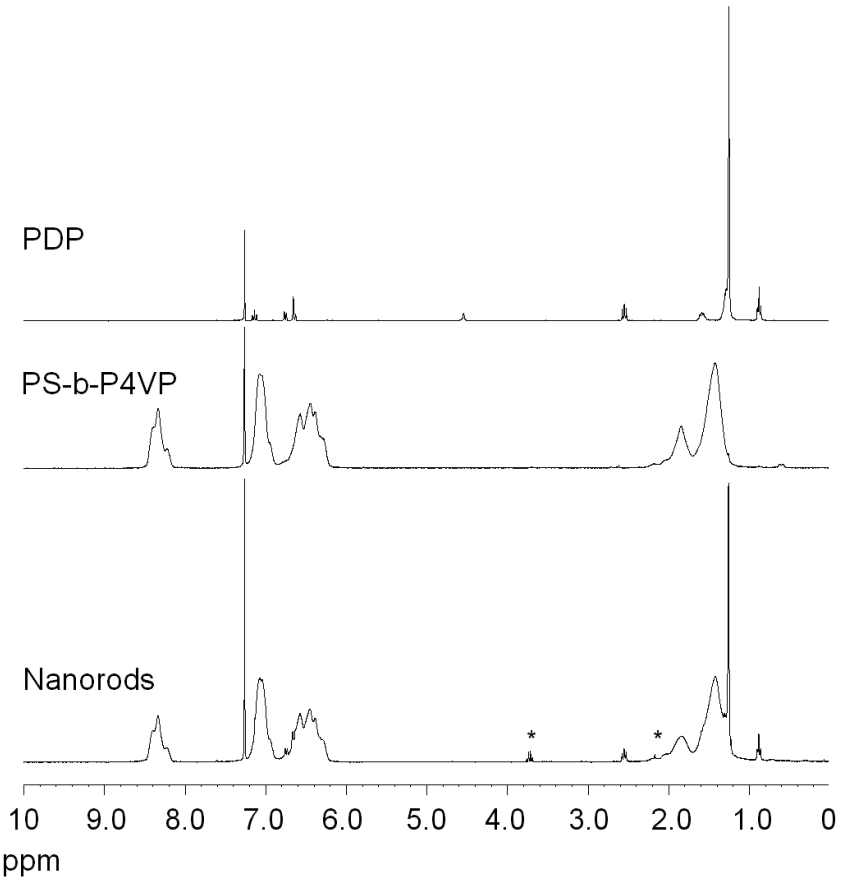

Figure 3.4. ^{1}H NMR to establish the presence of PDP in the nanorods. Peaks at 7.26 ppm are caused by the residual protons of chloroform-d. The peaks with an asterisk are due to residual ethanol.

conclude that in the P103(PDP) system, given its $T_g \cong 67$ °C, there will also be ~5% w/w PDP inside the PS layers. Comparing the increase in T_g as a function of PPE in the present case with that for the samples without PDP shows that the difference becomes larger for higher amounts of PPE, which indicates that in the P103(PDP)/PPE systems more PDP will be present in the PS/PPE layers for higher amounts of PPE. This conclusion is corroborated by several other observations. First, the ODT of the P4VP(PDP) phase decreases from ca. 57 °C for systems without PPE to ca. 52 °C for the higher PPE fractions. In pure homopolymer-based P4VP(PDP) systems, the ODT has been reported to drop to lower values for less than stoichiometric amounts (with respect to the number of pyridine groups) of PDP.[45,46] Furthermore, a decrease in the melting temperature of PDP can be observed as well, which again is an indication that PDP migrates toward the PS/PPE layers in an increasing extent for higher PPE fractions, since a lower mole fraction of PDP in the P4VP(PDP) complex results in lower crystallization temperatures for PDP.[41,47] The most important observation, however, is the gradual reduction in the enthalpy of melting from ca. 35 J g^{-1} PDP for the sample without PPE to ca. 25 J g^{-1} PDP for the sample with w_{PPE} = 0.40, which indicates that as much as 25% of the PDP present in the sample without PPE will have migrated to the PS/PPE layers for the sample with the highest amount of PPE.

3.3.2 Small Angle X-ray Scattering

The presence of a single composition dependent T_g of the PS/PPE layers is already sufficient evidence to conclude that PS and PPE are mixed throughout the PS layers. To study this further, SAXS was used to determine the dependence of the long period on the amount of PPE.

A simple theoretical model to describe the change in domain dimensions of a lamellar self-assembled block copolymer system on incorporation of nanoparticles inside one of the layers of a lamellar diblock copolymer was put forward by Hamdoun et al.[47] This description is not specific to nanoparticles but applies equally well to homopolymer/block copolymer blends, and recently it was used to discuss the distribution of low molar mass PS in the lamellae of thin films of nearly symmetric polystyrene-*block*-poly(methyl methacrylate) (PS-*b*-PMMA) diblock copolymers[48] and of polyvinylidene fluoride (PVDF) in the lamellae of thin films of similar PS-*b*-PMMA diblock copolymers.[49]

If the homopolymers segregate in the midplane, the chain conformations of the copolymer blocks and the distance between the copolymer junction points are not affected. Hence, a change will only occur in the direction perpendicular to the interface (Figure 3.5), and the domain

spacing L increases rapidly from its original value L_0 when homopolymer is added. As a result

$$L_o = L - \varphi L \quad \rightarrow \quad L = \frac{L_o}{1-\varphi} \tag{2}$$

with φ the volume fraction homopolymer in the entire system. When, on the other hand, the homopolymer chains are distributed uniformly throughout the A phase of lamellar self-assembled A-B diblock copolymer, the A blocks become even more stretched than is already the case under the strong segregation conditions assumed here. Part of this additional stretching is relieved by an increase in the average distance between junction points. At the same time the B blocks become somewhat less stretched in order to keep the segment density constant. The balance between these three effects leads to an L spacing which only slightly increases upon addition of homopolymer (Figure 3.6).

If the Alexander-De Gennes approximation is used to calculate the periodicity, it is found that

$$L = \frac{g(f,\varphi)^{-1/3}}{1-\varphi} L_0 \tag{3}$$

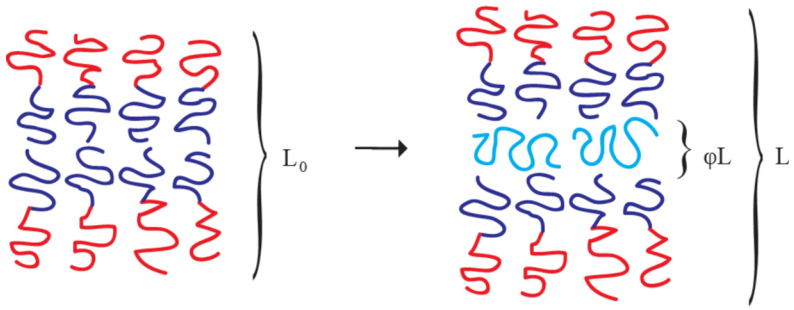

Figure 3.5. Schematic representation of homopolymer segregation in the midplane. The conformations of the blocks are not affected, and the domain spacing increases linearly with the addition of homopolymer.

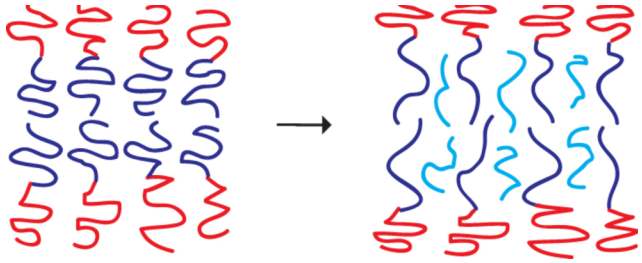

Figure 3.6. Schematic representation of uniformly distributed homopolymer. The A chains of the block copolymer are slightly more stretched after the addition of homopolymer. The distance between junction points is slightly larger, and the B-blocks are accordingly somewhat less stretched. The total L*-spacing increases only slightly.*

$$\text{with } g(f,\varphi) = \frac{f + (1-f)\varphi^2}{f(1-\varphi)^2} \tag{4}$$

and f the volume fraction A blocks (composition) of the diblock copolymer.[47] The assumption of a uniform distribution of homopolymer is in line with the Alexander-De Gennes approximation. A more accurate self-consistent-field approach will obviously show a slightly nonuniform homopolymer distribution with somewhat more homopolymer near the midplane where the copolymer blocks are least stretched. [25,30,50]

Figure 3.7 shows a graph of these theoretical predictions together with the experimental data for the symmetric diblock copolymer based P3546/PPE mixtures. Volume fraction was approximated by weight fraction as the densities of the two phases are only slightly different.[35] The experimental results closely follow the theoretical curve for a uniform distribution, even though the molar mass of the PPE homopolymer is larger than that of the PS block. As discussed above, in mixtures of A homopolymer with an AB diblock, A will only be distributed uniformly throughout the A lamellae if its molar mass is smaller than that of the corresponding block. Only short chains possess enough translational entropy to overcome the loss in conformational entropy caused by the stretching of the A blocks. The uniform distribution of PPE in mixtures of PPE and PS-*b*-P4VP is caused by the favorable interaction between PS and PPE. It confirms the conclusion reached before that this interaction is sufficiently strong to overcome the decrease in conformational entropy of the stretched PS chains, even for PPE of relatively high molar mass.[25,26]

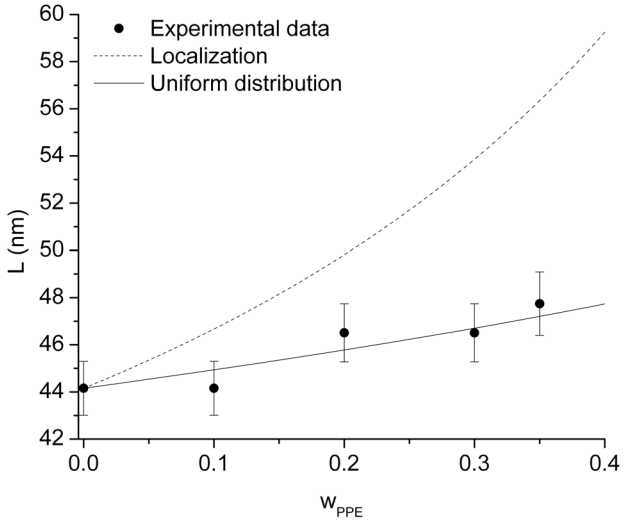

Figure 3.7. Lamellar period of P3546/PPE as a function of the weight fraction of PPE in PS/PPE. Theoretical predictions by equations (2) and (3), approximating volume by weight fraction, are also depicted.

The experimental results for the supramolecules-based P103(PDP)/PPE blends are presented in Figure 3.8. The theoretical curves are based on eqs 2 and 3, taking as L_0 the periodicity of the pure PS-*b*-P4VP(PDP) supramolecules system. The weight fraction of PPE in the PS/PPE layers used in Figure 3.8 is calculated on the basis of PPE and PS only, ignoring the additional presence of PDP. The experimental data indicate a stronger dependence of the long period on the amount of PPE added than the theoretical curve based on eq 3. It is tempting to attribute this deviation to the fact that the P4VP(PDP) layers, rather than involving linear chains, contain comb-shaped supramolecules. This difference in architecture will influence the adaptation of these blocks to the additional stretching of the PS blocks due to the addition of PPE. Of course, the fact that a fraction of the PDP resides in the PS/PPE layers, a fraction that moreover increases as a function of the amount of PPE added, is another complication. Still, the data clearly indicate that PPE is distributed throughout the PS phase; otherwise, the long period would have increased much faster as a function of the amount of PPE added. The situation is schematically illustrated in Figure 3.9.

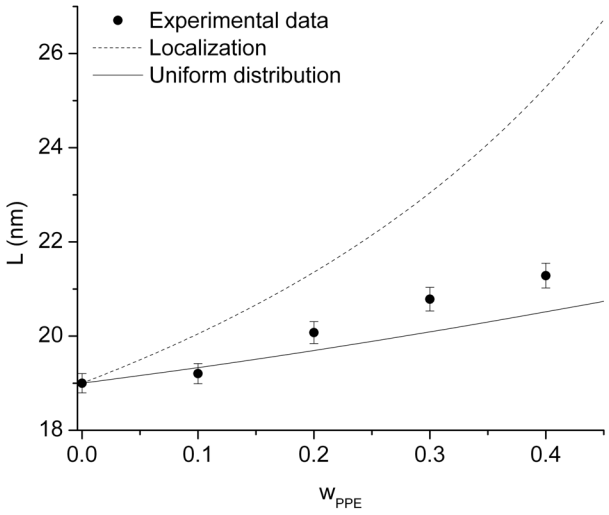

Figure 3.8. Lamellar period of P103(PDP)/PPE as a function of the weight fraction of PPE in PS/PPE. Theoretical predictions by equations (2) and (3), approximating volume by weight fraction, are again depicted.

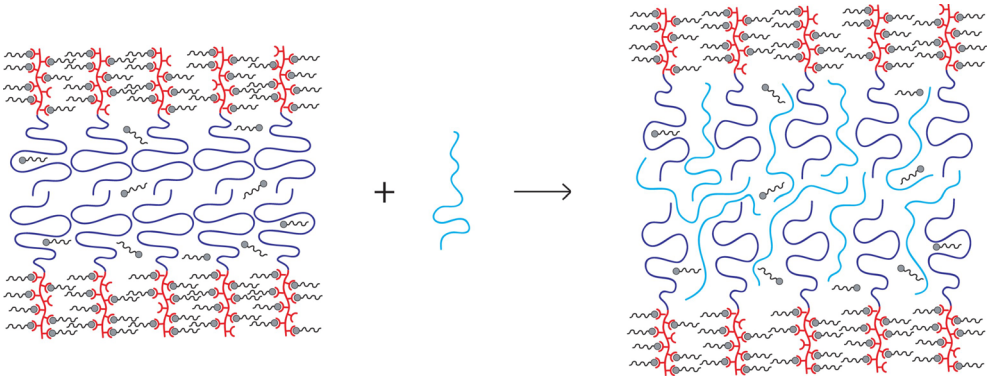

Figure 3.9. Schematic picture of self-assembled PS-b-P4VP(PDP) before and after incorporation of PPE.

3.4 Conclusion

The thermal properties and the lamellar periodicity in blends of PPE with PS-*b*-P4VP diblock copolymers and with PS-*b*-P4VP(PDP) diblock copolymer-based supramolecules were investigated by DSC and SAXS. DSC measurements of the PS-*b*-P4VP(PDP) demonstrated that PDP, though preferentially present in the P4VP layers, is also to some extent (ca. 5% w/w) present in the PS layers. The presence of PDP in PS domains was additionally confirmed by NMR on PS-*b*-P4VP core-corona nanorods produced from hexagonally ordered PS-*b*-P4VP(PDP) supramolecules. For PPE/PS-*b*-P4VP(PDP) blends the amount of PDP in the PPE/PS domains increases as a function of the amount of PPE added. The presence of PDP in the PPE/PS domains and the corresponding increased mobility is of direct interest for the large-amplitude oscillatory shear procedures that are used to induce macroscopic alignment in these systems.[19,33-35] In a completely different study on orientational switching of microdomains in hydrogen-bonded side-chain liquid-crystalline block copolymers by AC electric fields, Chao and co-workers[51] observed that the hydrogen-bonded mesogens were also partly present in the linear PS-block layers. As a consequence, the T_g of the PS layers was around 70 °C, and this plasticizing effect turned out to be essential for the fast orientational switching.

For both the block copolymer and the supramolecules blends, thermal analysis shows that PPE is distributed throughout the PS layers, even though the PPE chains have a higher molar mass than the PS blocks. Of course, there will be a composition profile of PPE inside the PS layers with a slight suppression at the interface, which may even be somewhat enhanced due to the interaction between PPE and P4VP being even more unfavorable than that between PS and P4VP,[36] and a slight excess near the midplane.[25,26]

The location of the PPE chains inside the PS lamellae was also investigated with SAXS by measuring the lamellar period as a function of the weight fraction of PPE. The fact that the long period increased only slightly as a function of the amount of PPE confirmed the conclusions drawn from thermal analysis.

In the previous chapter, blends of PPE and PS-*b*-P4VP(DDP) have been used to prepare core-corona nanorods with improved mechanical properties. Under the assumption that PPE mixes homogeneously with the PS blocks, it was estimated that the PS core of the nanorods should at least contain a critical weight fraction PPE of $w_{PPE} = 0.17$ in order that entanglements of PPE chains could be formed. In that study the same PPE batch was used. Experimentally, it turned out that a somewhat higher

amount of PPE was required to obtain the necessary strength for the nanorods to span the pores of ca. 200 nm of alumina ultrafiltration membranes. The present study confirms that the assumption of homogeneous PPE distribution, underlying the discussion in Chapter 2, is indeed to a good approximation satisfied.

3.5 References

1. F. S. Bates, G. H. Fredrickson, *Annu. Rev. Phys. Chem.* **1990**, *41*, 525-557.
2. M. Muthukumar, C. K. Ober, E. L. Thomas, *Science* **1999**, *277*, 1225-1232.
3. I. W. Hamley, *The physics of block copolymers*, Oxford Science publications, **1998**.
4. G. H. Fredrickson, F. S. Bates, *Phys. Today* **1999**, *52*, 32-38.
5. V. Abetz, P. F. W. Simon, *Adv. Polym. Sci.* **2005**, *189*, 125-212.
6. J.-M. Lehn, *Polym. Int.* **2002**, *51*, 825-839.
7. C.-Y. Chao, X. Li, C. K. Ober, *Pure Appl. Chem.* **2004**, *76*, 1337-1343.
8. I. W. Hamley, *Angew. Chem. Int. Ed.* **2003**, *42*, 1692-1712.
9. J. M. Pollino, M. Weck, *Chem. Soc. Rev.* **2005**, *34*, 193-207.
10. W. H. Binder, *Monatshefte für Chemie* **2005**, *136*, 1-19.
11. S. Förster, T. Plantenberg, *Angew. Chem. Int. Ed.* **2002**, *41*, 688-714.
12. O. Ikkala, G. ten Brinke, *Science* **2002**, *295*, 2407-2409.
13. O. Ikkala, G. ten Brinke, *Chem. Commun.* **2004**, 2131-2137.
14. G. ten Brinke, O. Ikkala, *Chem. Rec.* **2004**, *4*, 219-230.
15. M. Hillmyer, *Adv. Poly. Sci.* **2005**, *190*, 137-181.
16. T. Thurn-Albrecht, J. Schotter, G. A. Kästle, N. Emley, T. Shibauchi, L. Krusin-Elbaum, K. Guarini, C. T. Black, M. T. Tuominen, T. P. Russell, *Science* **2000**, *290*, 2126-2129.
17. G. Liu, J. Ding, *Adv. Mater.* **1997**, *9*, 437-439.
18. K. de Moel, G. O. R. Alberda van Ekenstein, H. Nijland, E. Polushkin, G. ten Brinke, R. Mäki-Ontto, O. Ikkala, *Chem. Mater.* **2001**, *13*, 4580-4583.
19. G. O. R. Alberda van Ekenstein, E. Polushkin, H. Nijland, O. Ikkala, G. ten Brinke, *Macromolecules* **2003**, *36*, 3684-3688.
20. O. Olabisi, L. M. Robeson, M. T. Shaw, *Polymer-Polymer Miscibility*, Academic Press, New York, **1979**.
21. G. R. Patzke, F. Krumeich, R. Nesper, *Angew. Chem.* **2002**, *41*, 2446-2461.
22. R. H. A. Ras, M. Kemell, J. de Wit, M. Ritala, G. ten Brinke, M. Leskelä, O. Ikkala, *Adv. Mater.* **2007**, *19*, 102-106.
23. H.-K. Lee, C.-K. Kang, W.-C. Zin, *Polymer* **1997**, *38*, 1595-1600.
24. J.-H. Ahn, B.-H. Sohn, W.-C. Zin, S.-T. Noh, *Macromolecules* **2001**, *34*, 4459-4465.
25. P. S. Tucker, J. W. Barlow, D. R. Paul, *Macromolecules* **1988**, *21*, 1678-1685.
26. P. S. Tucker, J. W. Barlow, D. R. Paul, *Macromolecules* **1988**, *21*, 2794-2800.
27. T. Hashimoto, K. Kimishima, H. Hasegawa, *Macromolecules* **1991**, *24*, 5704-5712.
28. T. Hashimoto, H. Tanaka, H. Hasegawa, *Macromolecules* **1990**, *23*, 4378-4386.

29. H. Tanaka, T. Hashimoto, H. Hasegawa, *Macromolecules* **1991**, *24*, 240-251.
30. K. I. Winey, E. L. Thomas, L. J. Fetters, *Macromolecules* **1991**, *24*, 6182-6188.
31. K. Shull, A. M. Mayes, T. P. Russell, *Macromolecules* **1993**, *26*, 3929-3936.
32. R. Mäkinen, J. Ruokolainen, O. Ikkala, K. de Moel, G. ten Brinke, W. De Odorico, M. Stamm, *Macromolecules* **2000**, *33*, 3441-3446.
33. K. de Moel, R. Mäkinen, M. Stamm, O. Ikkala and G. ten Brinke, *Macromolecules* **2001**, *34*, 2892-2900.
34. R. Mäkinen, K. de Moel, W. de Odorico, J. Ruokolainen, M. Stamm, G. ten Brinke and O. Ikkala, *Adv. Mater.* **2001**, *13*, 117-121.
35. J. Ruokolainen, M. Saariaho, O. Ikkala, G. ten Brinke, E. L. Thomas, M. Torkkeli, R. Serimaa, *Macromolecules* **1999**, *32*, 1152-1158.
36. J. de Wit, G. O. R. Alberda van Ekenstein, G. ten Brinke, *Polymer* **2007**, *48*, 1606-1611.
37. G. O. R. Alberda van Ekenstein, R. Meyboom, G. ten Brinke and O. Ikkala, *Macromolecules* **2000**, *33*, 3752-3756.
38. J. Ruokolainen, R. Mäkinen, M. Torkkeli, T. Mäkelä, R. Serimaa, G. ten Brinke, O. Ikkala, *Science* **1998**, *280*, 557-560.
39. J. Ruokolainen, G. ten Brinke, O. Ikkala, *Adv. Mater.* **1999**, *11*, 777-780.
40. M. C. Luyten, G. O. R. Alberda van Ekenstein, G. ten Brinke, J. Ruokolainen, O. Ikkala, M. Torkkeli, R. Serimaa, *Macromolecules* **1999**, *32*, 4404-4410.
41. P. R. Couchman, F. E. Karasz, *Macromolecules* **1978**, *11*, 117-119.
42. P. R. Couchman, *Macromolecules* **1978**, *11*, 1156-1161.
43. C. Mazard, L. Benyahia, J.-F. Tassin, *Polym. Int.* **2003**, *52*, 514-521.
44. L. An, D. He, J. Jing, Z. Whang, D. Yu, B. Jiang, Z. Jiang, R. Ma, *Eur. Polym. J.* **1997**, *33*, 1523-1528.
45. J. Ruokolainen, M. Torkkeli, R. Serimaa, B. E. Komanschek, O. Ikkala, G. ten Brinke, *Phys. Rev. E* **1996**, *54*, 6646-6649.
46. O. Ikkala, J. Ruokolainen, M. Torkkeli, J. Tanner, R. Serimaa, G. ten Brinke, *Coll. Surf. A* **1999**, *147*, 241-248.
47. B. Hamdoun, D. Ausserré, V. Cabuil, S. Joly, *J. Phys. II France* **1996**, *6*, 503-510.
48. K. A. Orso, P. F. Green, *Macromolecules* **1999**, *32*, 1087-1092.
49. S. I. Yoo, S.-H. Yun, J. M. Choi, B.-H. Sohn, W.-C. Zin, J. C. Jung, K. H. Lee, S. M. Jo, J. Cho, C. Park, *Polymer* **2005**, *46*, 3776-3781.
50. A. N. Semenov, *Sov. Phys. JETP* **1985**, *26*, 733-742.
51. C.-Y. Chao, X. Li, C. K. Ober, C. Osuji, E. L. Thomas, *Adv. Mater.* **2004**, *14*, 364-370.